

[Supporting Information]

Benzotrifuran-based donor-acceptor covalent organic frameworks for enhanced photocatalytic hydrogen generation

Chuanmeng Yang,^{a†} Zhenwei Zhang,^{a†} Jiali Li,^a Yuxin Hou,^a Qi Zhang*,^b Zhongping Li,^d Huijuan Yue,^c and Xiaoming Liu*^a

^a*College of Chemistry, Jilin University, Changchun, 130012, P.R. China.*

^b*School of Engineering, University of Warwick, Coventry CV4 7AL, UK*

^c*State Key Laboratory on Integrated Optoelectronics, College of Electronic Science and Technology, Jilin University, Changchun, 130012, P.R. China.*

^d*School of Energy and Chemical Engineering/Center for Dimension-Controllable Organic Frameworks, Ulsan National Institute of Science and Technology (UNIST), Ulsan, 44919, Republic of Korea.*

†These authors contributed equally to manuscript

Email address: xm_liu@jlu.edu.cn (X. Liu); 1033012429@qq.com (Q. Zhang)

Table of Content

Section 1. Material and Characterization

Section 2. Synthesis and Photocatalysis

Section 3. References

Section 1. Material and Characterization

Materials:

1,3,5-trifluorobenzene, Periodic acid, CsOH•H₂O and trifluoromethanesulfonic acid were purchased from Energy Chemical. L- ascorbic acid and trifluoromethanesulfonic were obtained from Macklin Chemical Reagent. Hydrogen hexachloroplatinate was obtained from Shanghai No. 1 Reagent Factory. The organic solvents obtained from Beijing Chemical Reagent and were distilled over appropriate drying reagents under nitrogen before used. Deuterated solvents for NMR measurement were obtained from Aladdin.

Characterization:

Infrared spectra. The Fourier transform infrared (FT-IR) spectra were tested from 400 to 4000 cm⁻¹ on an Avatar FT-IR 360 spectrometer by using KBr pellets.

Nuclear Magnetic Resonance Spectroscopy (NMR). The solid-state ¹³C CP/MAS NMR spectra was measured by Bruker AVANCE III 400 WB spectrometer with a CP contact time of 2 ms and a MAS rate of 5 kHz. The liquid NMR spectroscopy was recorded on Avance III-400 NMR spectrometer, and the chemical shift (δ, ppm) is measured with the TMS as the standard.

Transmission Electron Microscope. Transmission electron microscopy was tested by a Philips-FEI Tecnai G2 F20 S-TWIN microscope equipped with a field emission gun operating at 200 kV. The technical parameters are as follows: point resolution of

0.24 nm, high resolution STEM resolution of 0.2 nm, objective lens spherical aberration coefficient C_s of 1.2 mm, focal length of the objective lens of 1.7 mm, and maximum sample inclination $\pm 40^\circ$.

UV/Vis spectra. Solid UV/Vis spectra was tested from 200nm to 800 nm by using Shimadzu Corporation U-4100 Spectrophotometer. Liquid UV/Vis spectra was recorded on the Shimadzu Corporation UV-2700 Spectrophotometer within the wavelength range 200–800 nm.

Powder X-ray diffraction. Powder X-ray diffraction data was measured by the PANalytical BV Empyrean diffractometer by depositing powder by using glass as substrate, with the 2θ from 1.5° to 40° .

Thermogravimetric analysis. Under nitrogen atmosphere, thermogravimetric analysis (TGA) was recorded on the TA Q500 thermogravimeter by measuring the weight loss atmosphere from room temperature to 800°C . The sample was heated at a rate of $10^\circ\text{C min}^{-1}$.

Nitrogen sorption isotherms. The Brunauer-Emmett-Teller (BET) method was used to estimate the specific surface areas and pore volume of sample with ASAP 2020 as analyzer. The sample was dried in vacuum at 80°C for more than 10 hours before measurement. The nonlocal density functional theory (NLDFT) method was applied for the estimation of pore size distribution.

Photoluminescence spectrum (PL). The PL spectrum were recorded on FLS920 Edinburgh Instrument. The activation wavelength of COF-JLU42 and COF-JLU32

were 360 nm and 380 nm, respectively. The E_b was measured by temperature-dependent photoluminescence technology, from which the E_b can be estimated from the integral emission intensity by fitted with equation (1):

$$I(T) = \frac{I_0}{1 + Ae^{-E_B/k_B T}} \quad (1)$$

where I_0 is the integral intensity at 0 K, E_B is the E_b , and k_B is the Boltzmann constant^[1].

Electron Paramagnetic Resonance (EPR). The electron paramagnetic resonance (ESR) spectra were recorded on the JEOL JES-FA200 ESR spectrometer, All the samples were measured at scanning frequency: 9229.871 MHz; scanning power: 0.998 mW; central field: 329.4 mT; scanning width: 50 G; scanning temperature: 298 K. The 300W Xe lamp with 420 nm cut-off filter was used to illuminate samples.

Photoelectrochemical measurements. All the photoelectrochemical measurements of samples were recorded on the electrochemical workstation (CHI760E, CH Instrument Corp, Shanghai) using a standard three-electrode cell at room temperature, the glass carbon electrode (GCE) were used as working electrode, a platinum wire electrode, and a saturated calomel electrode (SCE) as counter and reference electrode, respectively.

For Mott-Schottky analysis, a glassy carbon electrode covered with a thin polymer film and 5 wt% Nafion was applied as the working electrode, 0.1 M Na_2SO_4 aqueous solution was used as the electrolyte and Mott-Schottky measurement was carried out at frequency of 1000 Hz, 1500 Hz and 2000 Hz with amplitude of 5 mV.

For electrochemical impedance spectra (EIS) measurement, 0.1 M KCl solution containing 5 mM $[\text{Fe}(\text{CN})_6]^{3-/4-}$ was used as the electrolyte, 7 μL of slurry (5 mg powder, 225 μL deionized water, 225 μL EtOH and 50 μL 1.5 wt% PVDF NMP solution) was covered to GCE as working electrode.

The applied potential vs. saturated calomel electrode is converted to NHE or RHE potentials using the following equations:

$$E_{\text{NHE}} = E_{\text{SCE}} + E_{\text{SCE}}^{\theta} (E_{\text{SCE}}^{\theta} = 0.242 \text{ V}) \quad (1)$$

$$E_{\text{RHE}} = E_{\text{SCE}} + 0.0591\text{pH} + E_{\text{SCE}}^{\theta} (E_{\text{SCE}}^{\theta} = 0.242 \text{ V}) \quad (2)$$

For photocurrent measurement, the sample was illuminated by a 300W xenon lamp (CEAULIGHT, CEL-HXF300) with AM 1.5G cut-off filter and chopped manually. 5 mg of powder was added into 1 mL EtOH and 10 μL Nafion of 5 wt%, then ultrasonicated over 30 min to get slurry, 7 μL of slurry was further dispensed onto GCE glass and air drying. The electrolyte was 0.1 M Na_2SO_4 (pH = 6.8). The photocurrent measurements were recorded at -0.64 V (vs. SCE) for 800 s under intermittent irradiation with a period of 50 s.

Structure modelling. Structural modeling and Pawley refinement were carried out in the Materials Studio 2018 software package for crystal determination from XRD pattern. The space groups were obtained from the Reticular Chemistry Structure Resource. The theoretical models were then optimized by the Forcite module. Pawley refinements of the PXRD patterns were performed in the Reflex module from 2° to 40° , which are agreeable with the simulated patterns of AA stacking models.

DFT calculations. Density functional theory (DFT) calculations were carried out using QUANTUM ESPRESSO. Norm-conserving pseudopotentials from Pseudo-dojo project were used and their recommended energy cutoffs were employed for the planewave basis. A $3 \times 3 \times 2$ grid was used for Brillouin zone sampling. The calculations of macromolecule and cell were carried out using DFTB+ with mio parameter set.

Photocatalytic hydrogen evolution

COF-JLU42 (5 mg) was well dispersed in 50 mL of deionized water containing 0.1 M ascorbic acid (AA) as the sacrificial agent. Then 78 μL of 0.01 M chloroplatinic acid (H_2PtCl_6) aqueous solution (3 wt% Pt) was introduced into the reaction system. The reaction solution was evacuated under vacuum over 30 min to completely discharge air and maintained at 6 $^\circ\text{C}$ with a cooling jacket in the circulating cooling system. After that the reaction system was irradiated vertically under 300W xenon lamp with > 420 nm cut-off filter (160 mW cm^{-2}). or AM 1.5G (CEL-SPH2N, Beijing China Education Au-light Technology Co., Ltd.). The average rate obtained by photocatalysis for five hours included one hour of in-situ photodeposition. For recycled experiment, 5 mg COF-JLU42 was adopted with 50 mL deionized water containing 0.1 M AA (3 wt% Pt) and radiated under 300W xenon lamp with > 420 nm cut-off filter. In situ photodeposition was used in all experiments, 1 h for AA.

The evolved gases were analyzed by gas chromatography equipped with Ar as the carrier gas (GC7920, TDX01 chromatographic column, CEAULIGHT). The evolved hydrogen was detected with a thermal conductivity detector (TCD) referencing against high-purity hydrogen with a known volume. The catalyst and solution sprayed on the reactor wall are neglected, hydrogen dissolved in the reaction solution was not detected and measured. In addition, the effect of changed pressure by generated hydrogen on photocatalysis was ignored. The hydrogen evolution rates were calculated on the basis of a linear regression fitting curve ($R^2 = 0.9996$), the value of the rate curve excludes the Pt photodeposition period. As a comparison, COF-JLU32 was carried out H₂ evolution performance under the same conditions.

The apparent quantum yield (AQY) measurements

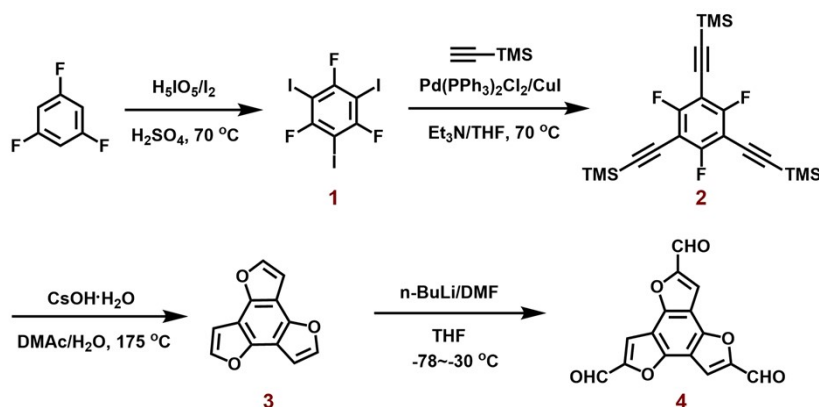
The test of apparent quantum yield (AQY)^[2] for hydrogen evolution was similar to photocatalytic hydrogen evolution measurement but a 300 W Xe lamp with different bandpass filters (central wavelength: 420, 450, 500, 550nm) was used as the source of light. Universally, 10 mg COF-JLU42 was employed accompanying with 50mL deionized water containing 0.1 M AA (3 wt% Pt). The intensities of incident light were measured by CEL-NP2000 optical power meter respectively, while the average intensity of irradiation was determined to be 11.7 mW cm⁻² at 450 nm. So the AQY was calculated can be calculated by using the following equation.

$$\begin{aligned}
 \text{AQY}(\%) &= \frac{\text{number of product obtained}}{\text{number of incident photons}} \times 100\% \\
 &= \frac{n_p \times N_A}{\frac{P \times S \times t \times \lambda}{h \times c}} \times 100\% \\
 &= \frac{n_p \times N_A \times h \times c}{P \times S \times t \times \lambda} \times 100\%
 \end{aligned}$$

where n_p is the mole number of product obtained (mol), N_A is the Avogadro constant ($6.022 \times 10^{23} \text{ mol}^{-1}$), P is the optical density (W cm^{-2}), S is the light irradiation area (18.1 cm^2), t is the light irradiation time (s), λ is the monochromatic light wavelength (m), h is Planck's constant ($6.626 \times 10^{-34} \text{ J s}$), and c is the speed of light ($3 \times 10^8 \text{ m s}^{-1}$).

Section 2. Synthesis and Photocatalysis

Synthesis of Benzo[1,2-b:3,4-b':5,6-b'']trifuran-2,5,8-tricarbaldehyde



Synthesis of compound 1: The periodic acid (2.93 g, 12.8 mmol) was added to concentrated H₂SO₄ (30 mL) and stirred until the solution became clear. Then I₂ (10.2 g, 40 mmol) was added in batches. The dark reaction system was stirred and cooled in an ice bath for 30 min. 1,3,5-trifluorobenzene (1.0 g, 7.58 mmol) was added over 10 min by syringe. The ice bath was removed and the solution was heated to 70 °C for 48 h. After completion of the reaction, the system was cooled to room temperature and poured into ice-water mixture slowly, and extracted with Et₂O (50 mL × 3). The organic phase was washed with conc. aq. Na₂S₂O₃ until the solution became colorless, dried over MgSO₄, and concentrated under reduced pressure. The crude product was purified by column chromatography (SiO₂, petroleum ether as the eluent) to afford compound 2 (2.5 g, 4.17 mmol, yield: 55%) as a white solid. ¹³C NMR (CDCl₃, 100 MHz): δ 63.9, 161.0, 163.4 ppm.

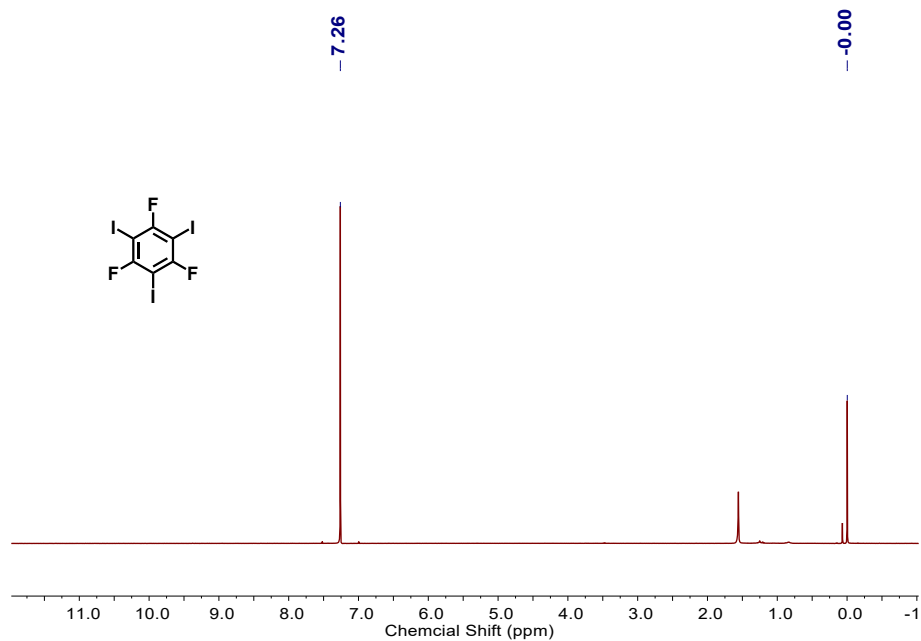
Synthesis of compound 2^[3]: Pd(PPh₃)₂Cl₂ (0.18 g, 0.23 mmol), CuI (0.094 g, 0.49 mmol) and compound 1 (2.5 g, 4.17 mmol) were added to a dry three-necked flask. Anhydrous and oxygen-free triethylamine (40 mL) was added under nitrogen atmosphere. Trimethylsilyl acetylene (1.94 mL, 13.6 mmol) was added dropwise via a syringe. After stirring for 30 min, anhydrous and oxygen-free tetrahydrofuran (40

mL) was added to the reaction system, which was then heated at 70 °C overnight. After completion of the reaction, the mixture was cooled to room temperature and filtered under reduced pressure and the cake was washed by petroleum ether. The organic phase was combined and passed through a rotary evaporator to remove the solvent. The crude product was purified by column chromatography (SiO₂, petroleum ether as the eluent) and then recrystallized from hexane to afford 1.5 g (3.54 mmol, yield: 85%) of target product as white needles. ¹H NMR (CDCl₃, 400 MHz): δ 0.26 (s, 12H) ppm. ¹³C NMR (CDCl₃, 100 MHz): δ 0.3, 88.5, 99.3, 106.7, 161.6, 164.2 ppm.

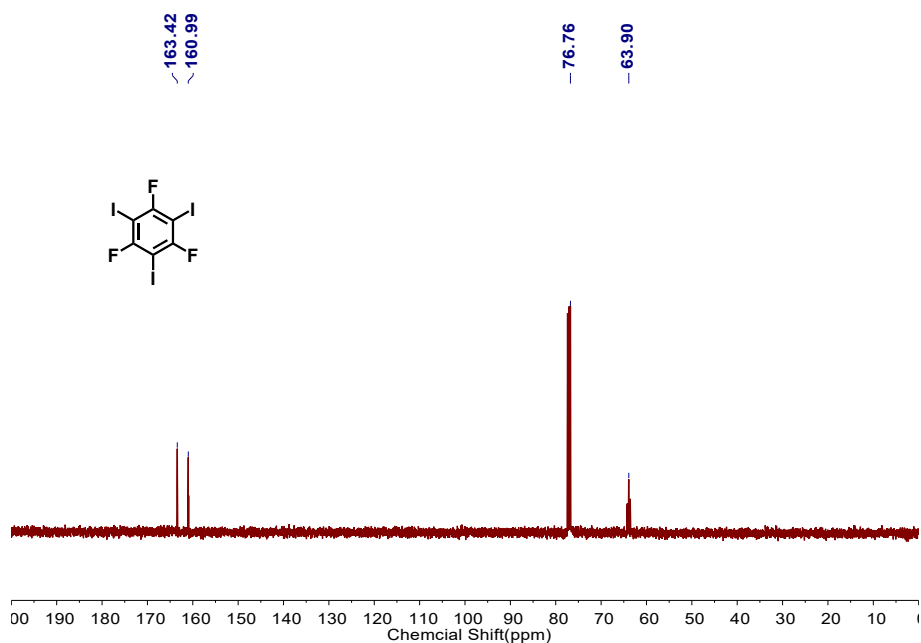
Synthesis of compound 3^[3]: Compound **2** (1.20 g, 2.86 mmol), CsOH•H₂O (4.72 g, 28.11 mmol) was dissolved in N,N-Dimethylacetamide (30 mL). Water (540 μL, 5.0 mmol) was added to the mixture and the reaction system was refluxed at 175 °C for 12 h. After completion of the reaction, the mixture was added by water (30 mL) and extracted with ethyl acetate (4 × 25 mL). The combined organic layers were dried over MgSO₄ and concentrated under reduced pressure. The crude product was purified by flash column chromatography on silica gel using petroleum ether as the eluent to afford 280 mg (1.41 mmol, 47% yield) of compound **3** as a white solid. ¹H NMR (CDCl₃, 400 MHz): δ 7.13 (s, 3H), 7.72 (s, 3H) ppm. ¹³C NMR (CDCl₃, 100 MHz): δ 103.7, 109.1, 143.5, 146.5 ppm.

Synthesis of compound 4: Compound **3** (198 mg, 1 mmol) and tetrahydrofuran (30 mL) was added to a dry ampoule under a nitrogen atmosphere. The ampoule was then placed in a low temperature bath. After cooled to -78°C, n-butyllithium solution (2.5 ml, 6.25 mmol, 2.5 mol L⁻¹) was added dropwise. The temperature was raised to -30 °C slowly. After reacting for 6 h, the temperature was lowered again to -78 °C and dry DMF (0.6 mL) was added dropwise. The reaction vial was removed from the cryogenic bath and brought to room temperature for 3 h. The mixture was then transferred to a saturated ammonium chloride solution and the water phase was extracted by CH₂Cl₂ at least five times. The organic layers were washed by saturated

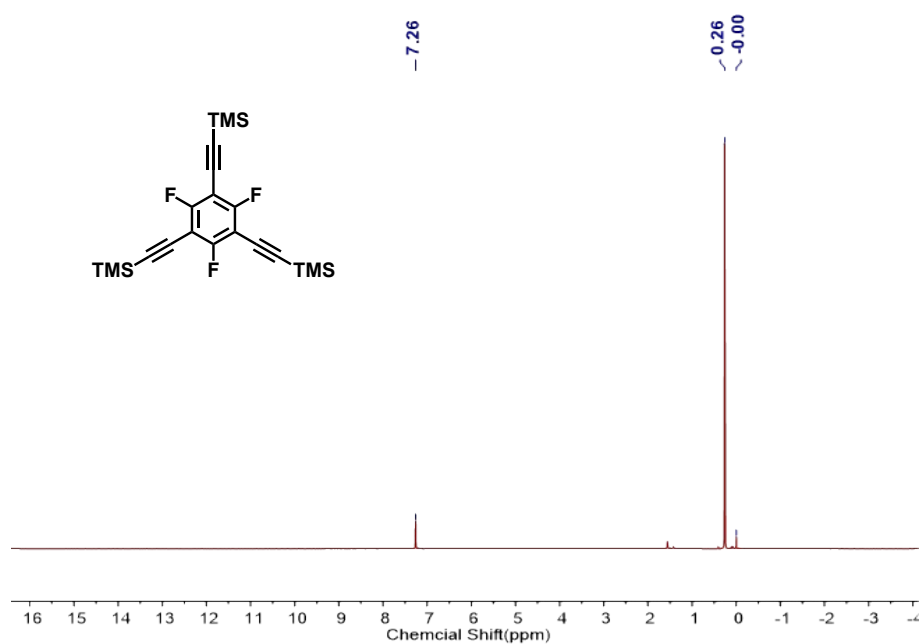
sodium chloride solution, dried over Na_2SO_4 and passed through a rotary evaporator to remove the solvent. The crude yellow product was purified by silica gel chromatography (DCM/ethyl acetate: 20/1) to give a pale yellow solid product. Yield: (87 mg, 31%). ^1H NMR (DMSO, 400 MHz): δ 8.6 (s, 3H), 9.9 (s, 3H) ppm.



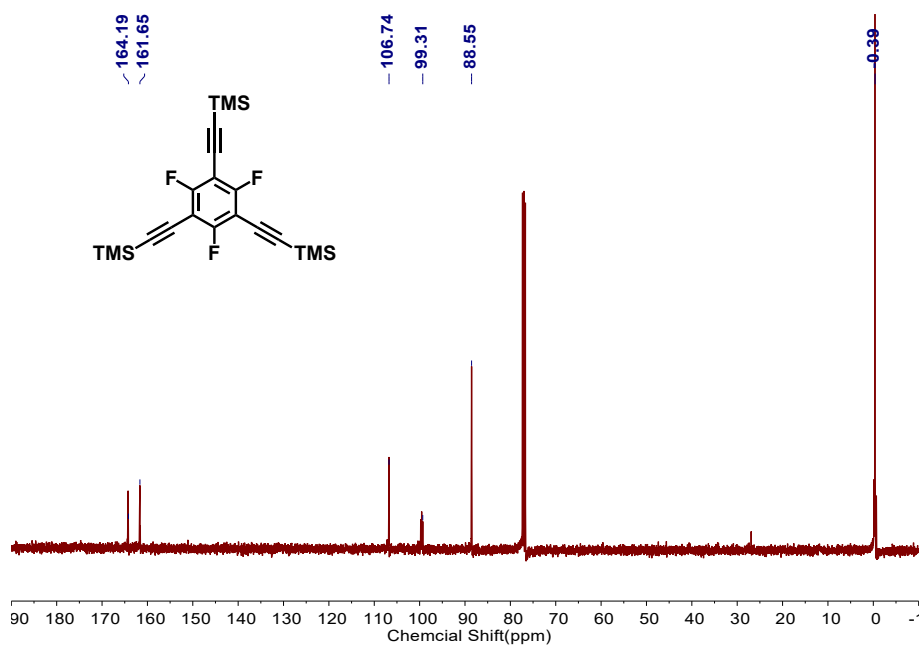
^1H NMR spectrum of compound 1.



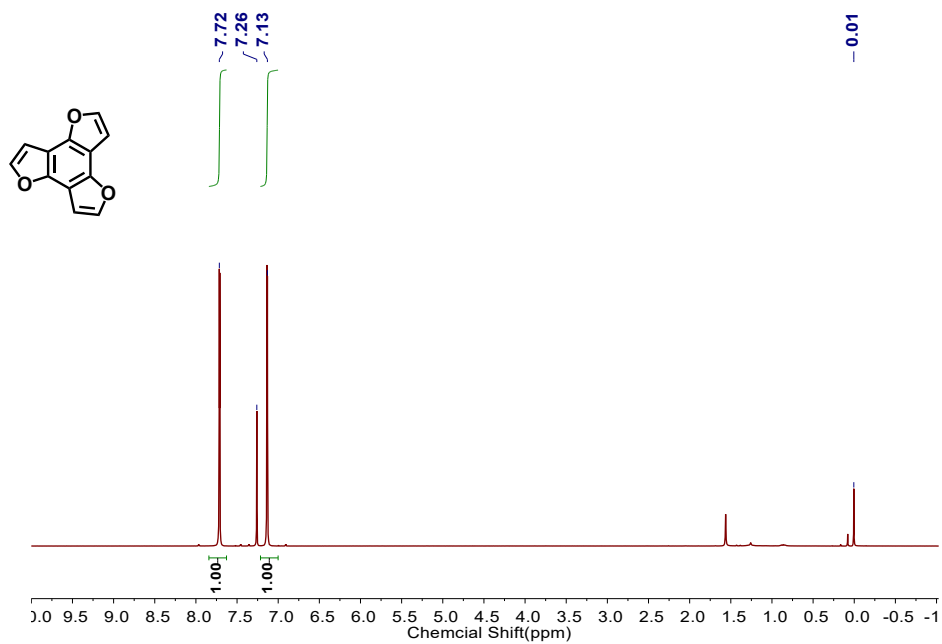
¹³C NMR spectrum of compound 1.



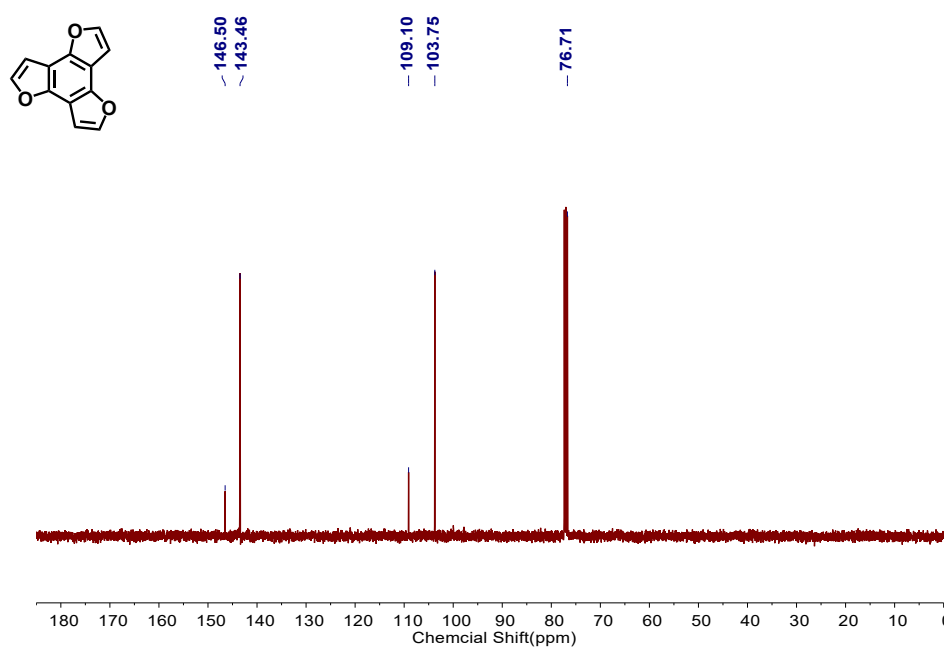
¹H NMR spectrum of compound 2.



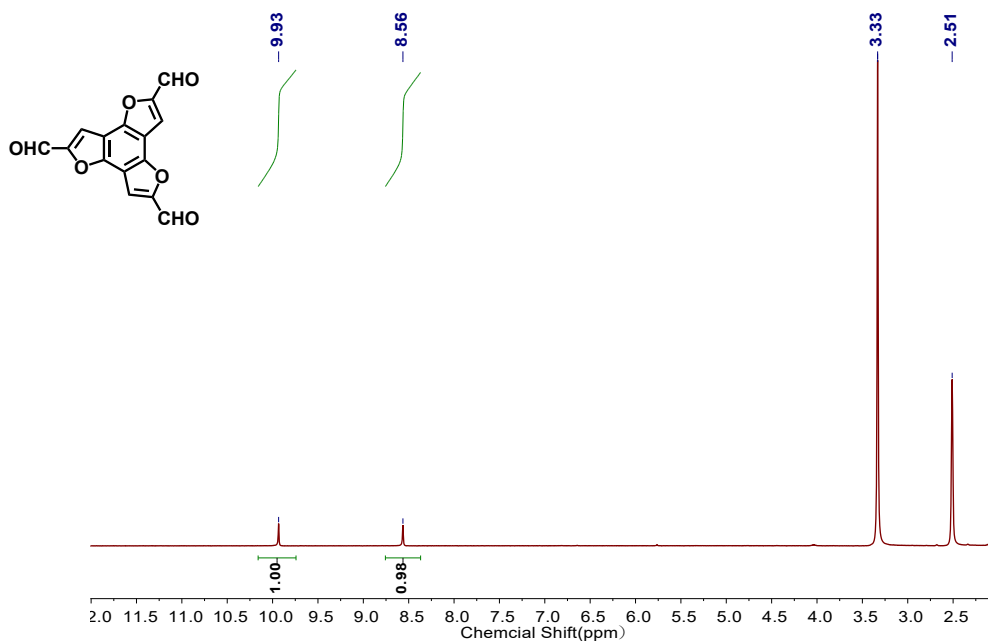
¹³C NMR spectrum of compound 2.



¹H NMR spectrum of compound 3.

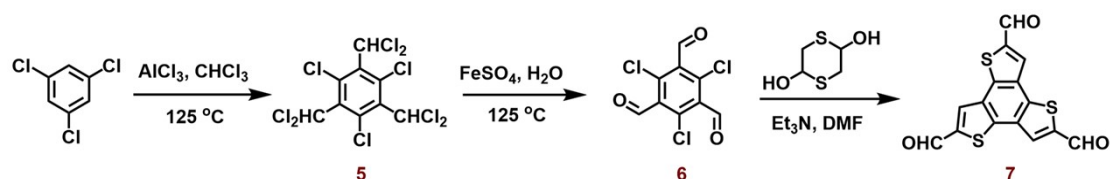


¹³C NMR spectrum of compound 3.



^1H NMR spectrum of compound **4**.

Synthesis of benzo[1,2-*b*:3,4-*b'*:5,6-*b''*]trithiophene

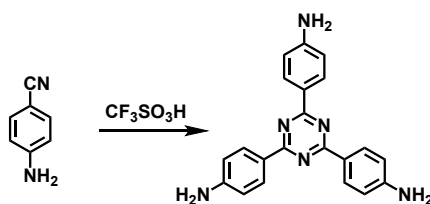


Synthesis of compound **5**^[4]: 1,3,5-trichlorobenzene (1.5 g, 8.25 mmol), aluminium chloride (1.3 g, 9.75mmol) and trichloromethane (30 mL) were added to a 50 mL polytetrafluoroethylene lined reactor which was then heated at 125 °C for 72 h. After completion of the reaction, the reaction system must to be cooled to room temperature and then poured into ice water. After stirring for 1 h, the mixture was extracted with dichloromethane. The combined organic phase was washed with saturated sodium chloride solution and dried over Na_2SO_4 . After concentration, the crude product was purified by flash column chromatography on silica gel using petroleum ether as the eluent to afford 1,3,5-trichloro-2,4,6-tris(dichloromethyl)benzene **5** (2.78 g, 78%) as a white solid. ^1H NMR (400 MHz, CDCl_3): δ 7.75 (s, 2H), 7.63 (s, 1H) ppm.

Synthesis of compound 6^[4]: 1,3,5-trichloro-2,4,6-tris(dichloromethyl)benzene (2.64 g, 6.14 mmol), FeSO₄ (120 mg, 0.80 mmol) and concentrated sulfuric acid (16 mL) was added to a 50 ml three-necked flask, which was then heated at 125 °C overnight. After completion of the reaction, the mixture was added to ice water slowly and stirred for 30min. The water phase was extracted by CH₂Cl₂ and the organic phase was combined and concentrated under reduced pressure. The crude product was chromatographed on silica gel with petroleum ether to get a white solid (0.88 g, 54.0%). ¹H NMR (400 MHz, CDCl₃): δ 10.42 (s, 3H) ppm.

Synthesis of compound 7^[4]: 2,4,6-trichlorobenzene-1,3,5-tricarbaldehyde (320 mg, 1.2 mmol), pdithiane-2,5-diol (274 mg, 1.8 mmol) and anhydrous DMF (5 mL) was added to a 50 mL three-necked flask. The mixture was added triethylamine (1 mL, 7.2 mmol) dropwise in the ice bath. After stirring for 10 min, the reaction system was heated at 35 °C overnight. It was poured into ice water after completion of reaction. The system was centrifuged and the solid was washed with water and THF, repeatedly. Finally, the target product was obtained as a pale brown solid with 71.6% yield.

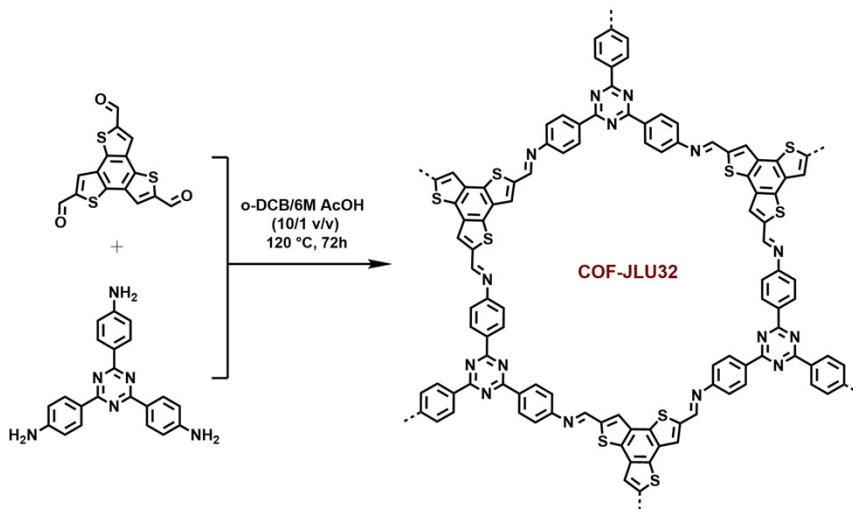
Synthesis of 2,4,6-tris(4-aminophenyl)-1,3,5-triazine^[5]



4-aminobenzonitrile (2 g, 8.29mmol) and CHCl₃ (60 mL) was added to a 150 mL three necked flask, which was then cooled to 0 °C in ice water bath. The trifluoromethanesulfonic acid (3 mL) was added dropwise to the flask. After stirring for 1h, the system was allowed to warm to room temperature and stirred for 72h. After completion of reaction, the mixture was added with 40 mL of water and then neutralized by an aqueous NaOH solution. The mixture was filtrated under reduced pressure, and the residue was washed with distilled water and MeOH to afford a pale

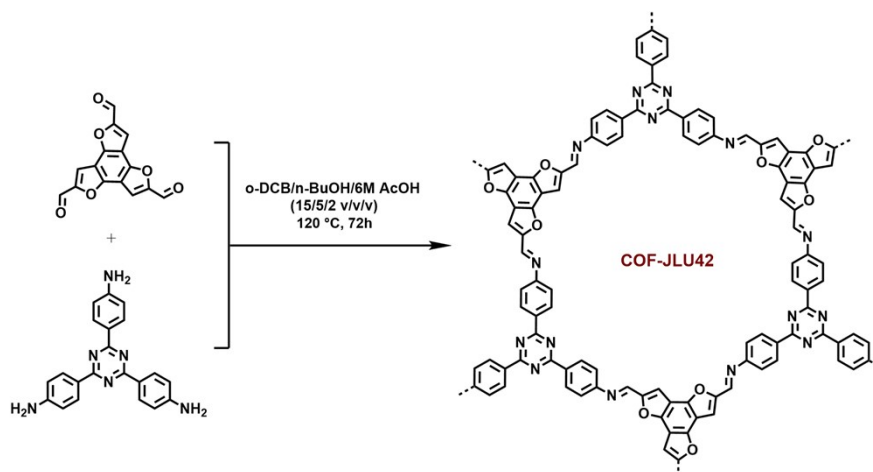
yellow solid. $^1\text{H NMR}$ (400 MHz, DMSO-d_6): δ 8.36 (d, 6H), 6.70 (d, 6H), 5.90 (s, 6H).

Synthesis of COF-JLU32



To a 5 ml reaction tube containing a mixture of benzo[1,2-b:3,4-b':5,6-b'']trithiophene-2,5,8-tricarbaldehyde (20 mg, 0.06 mmol), 2,4,6-tris(4-aminophenyl)-1,3,5-triazine (23mg, 0.06 mmol) was added o-dichlorobenzene (3 mL) and 6M HOAc (0.3 mL), which was degassed three times. After flame-sealing, the mixture was heated at 120 °C for 3 d, a orange powder was collected by centrifugation, washed with tetrahydrofuran (3×5 mL) and acetone (3×5 mL). The solid was gathered and dried at 100 °C in vacuum to produce COF-JLU32 with 75% isolated yield.

Synthesis of COF-JLU42



To a 3 ml reaction tube containing a mixture of benzo[1,2-b:3,4-b':5,6-b'']trifuran-2,5,8-tricarbaldehyde (11.4 mg, 0.04 mmol), 2,4,6-tris(4-aminophenyl)-1,3,5-triazine (14.2 mg, 0.04 mmol) was added o-dichlorobenzene (0.75 mL), 1-butanol (0.25 mL) and 6 M HOAc (0.1 mL), which was degassed three times. After flame-sealing, the mixture was heated at 120 °C for 3 d, a yellow powder was collected by centrifugation, washed with tetrahydrofuran (3 × 5 mL) and acetone (3 × 5 mL). The solid was gathered and dried at 100 °C in vacuum to produce COF-JLU42 with 90% isolated yield.

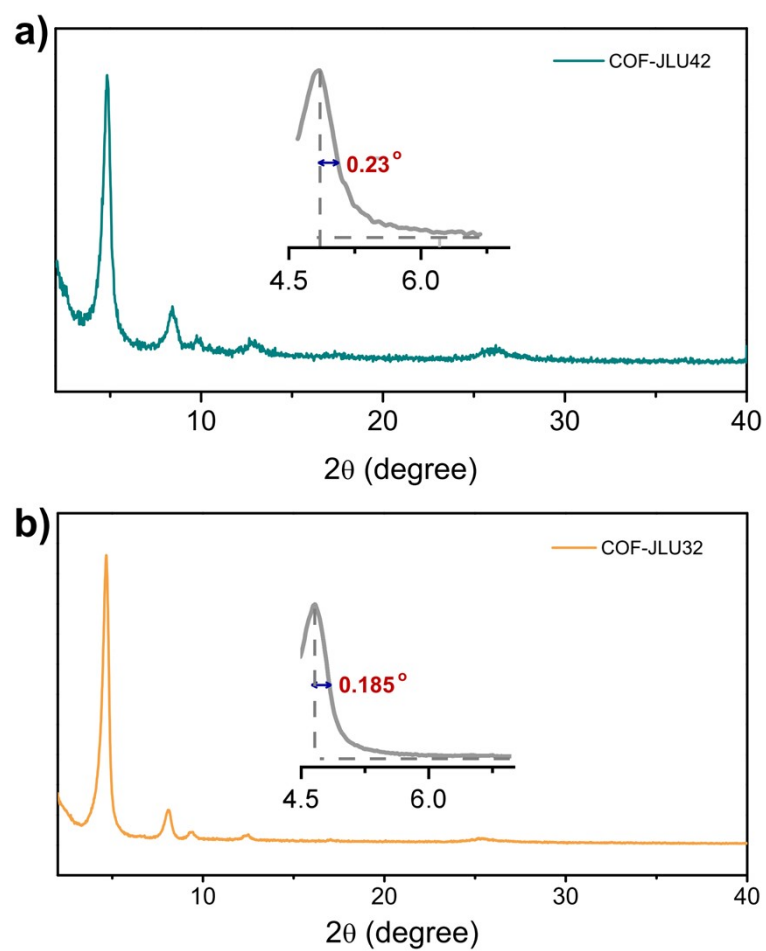


Figure S1. (a) PXR D spectra of COF-JLU42 (**FWHM** = $2 \times 0.23^\circ = 0.46^\circ$). (b)

PXR D spectra of COF-JLU32 (**FWHM** = $2 \times 0.185^\circ = 0.37^\circ$).

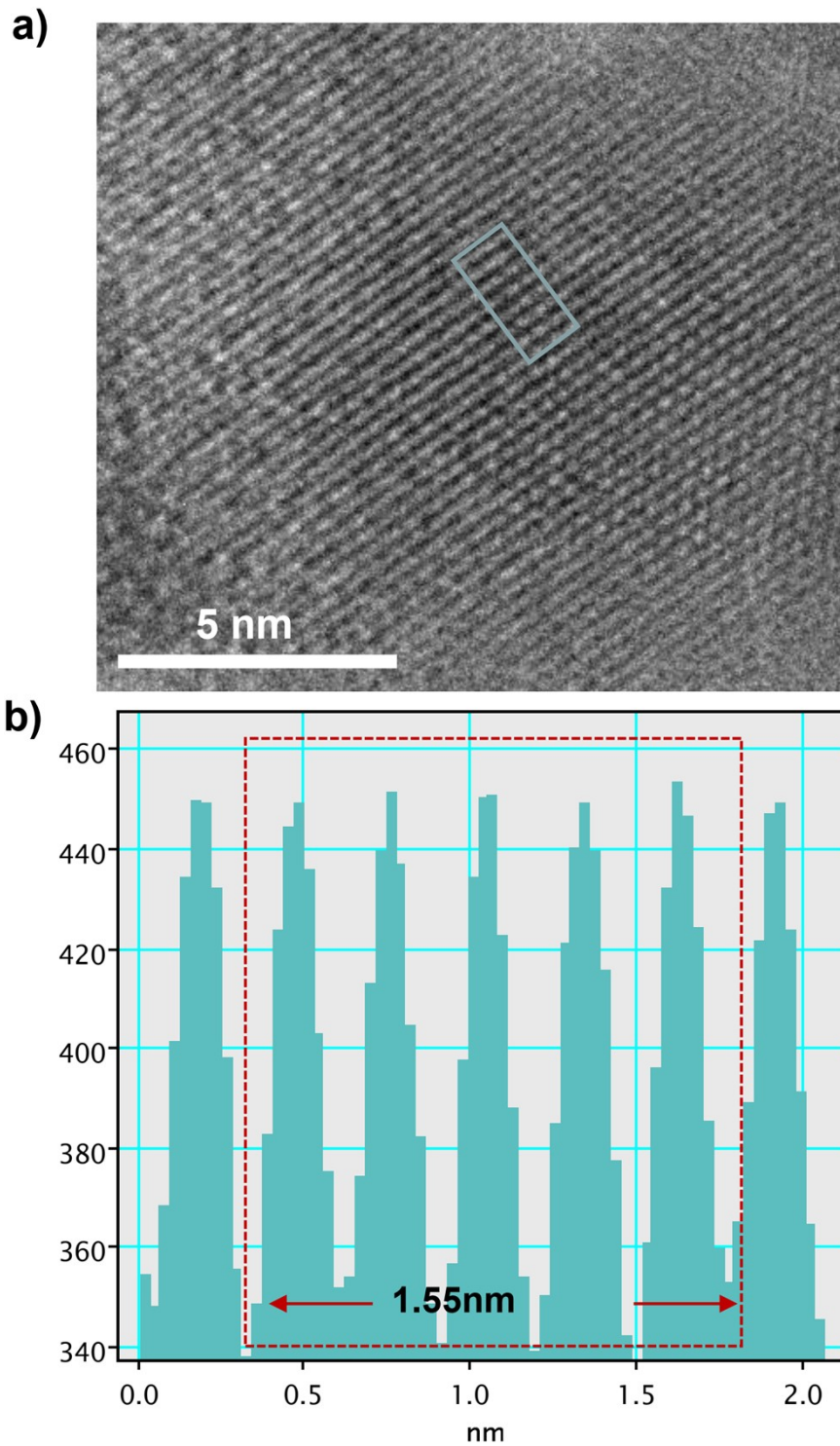


Figure S2. (a) The magnified HR-TEM image of COF-JLU42. (b) Rectangle profile along the indicated area in HR-TEM (the average distance from layer to layer is ~ 0.31 nm).

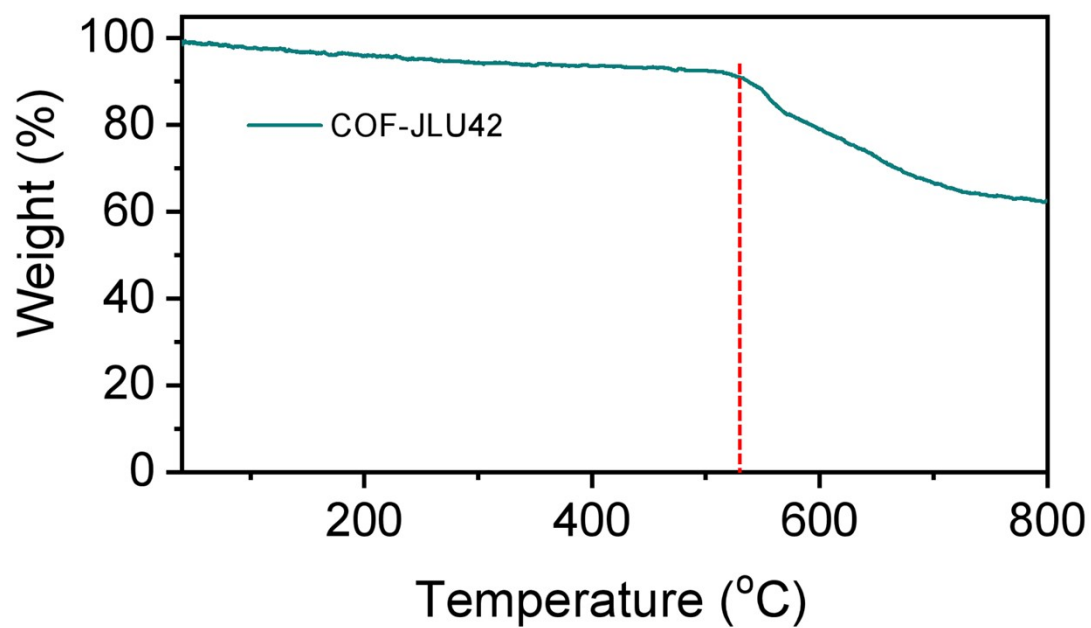


Figure S3. Thermogravimetric curves of COF-JLU42 under nitrogen atmosphere.

TGA analysis indicates that COF-JLU51 is thermally stable up to 520 °C under nitrogen atmosphere.

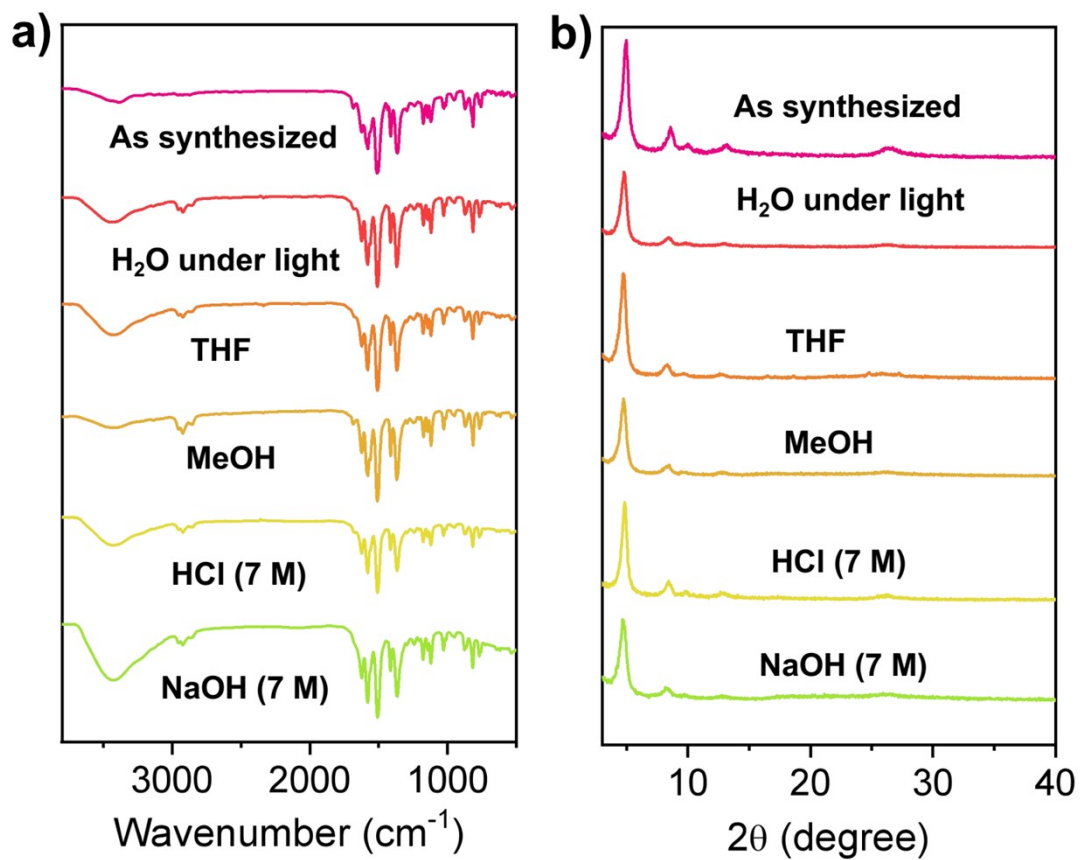


Figure S4. (a) PXRD curves and (b) FT-IR spectra of COF-JLU42 after treatment in different conditions for 3d.

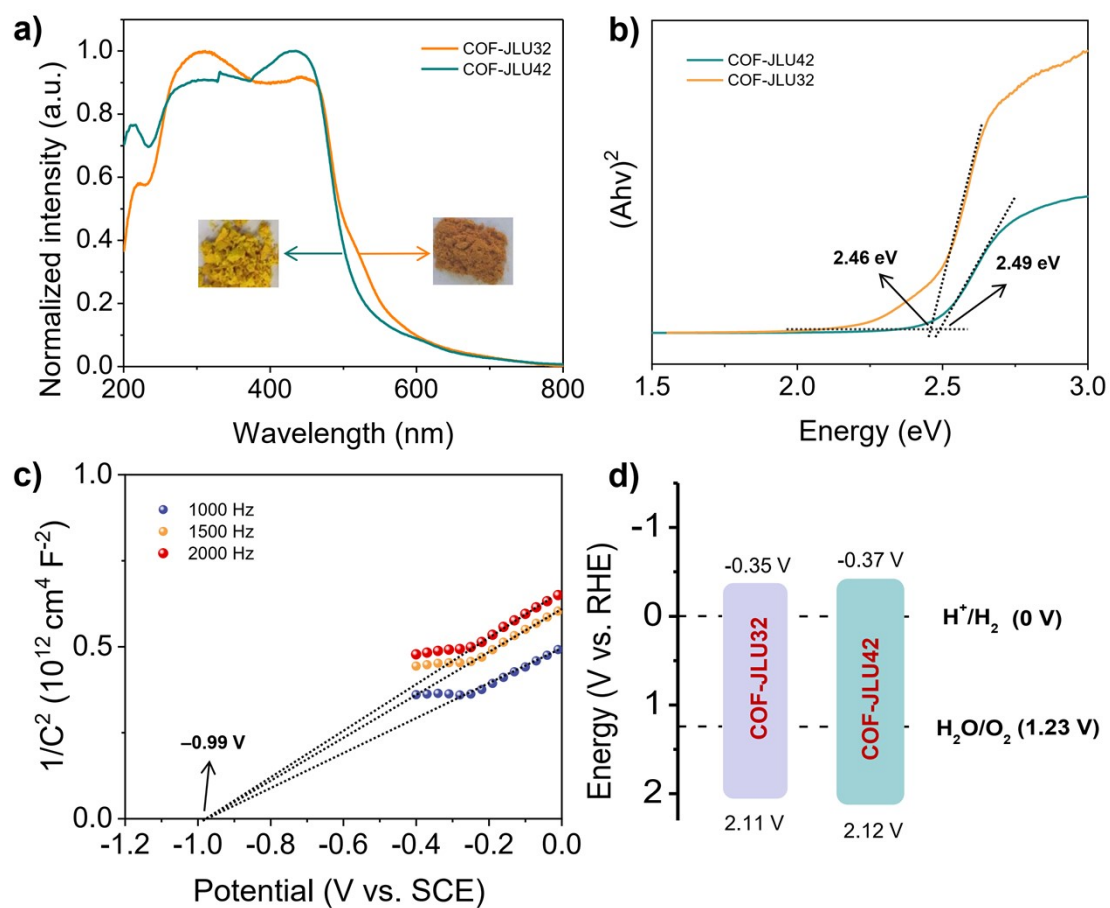


Figure S5. (a) UV-vis DRS pattern of COF-JLU42 and COF-JLU32. (b) The Tauc plots of COF-JLU42 and COF-JLU32. (c) Mott-Schottky plots of COF-JLU32. (d) Band structures diagram of COF-JLU42 and COF-JLU32 (the electrochemical potential at pH = 6.8, 0.1 M Na₂SO₄).

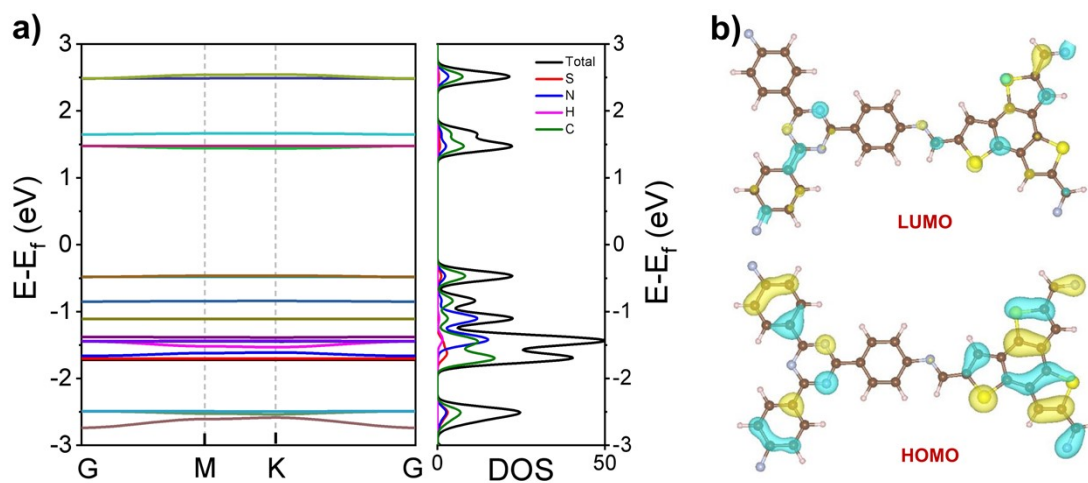


Figure S6. (a) Calculated band structure and density of states for COF-JLU32. (b) Kohn–Sham orbitals of LUMO and HOMO of COF-JLU32 (yellow: the positive phase of molecular orbital wave function, blue: the negative phase of molecular orbital wave function).

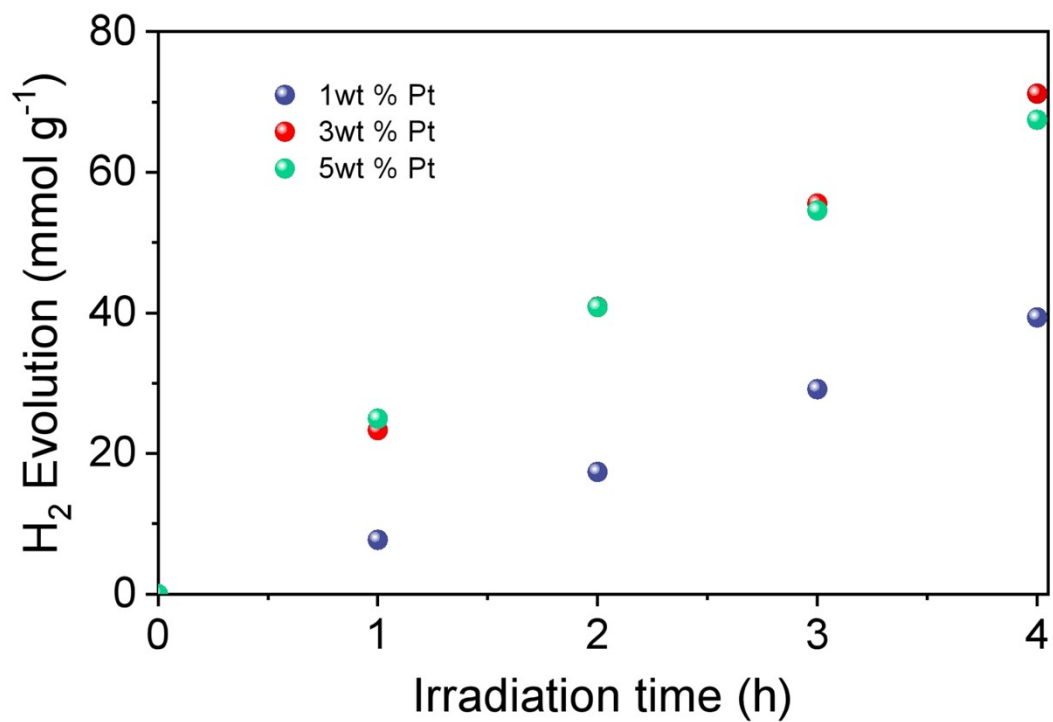


Figure S7. The hydrogen evolution curve of different Pt amount for COF-JLU42 in the optimized reaction conditions (5 mg of COF-JLU42, 50 mL of H₂O, 3 wt% Pt, 0.1 M AA as SED, $420 < \lambda < 780$ nm).

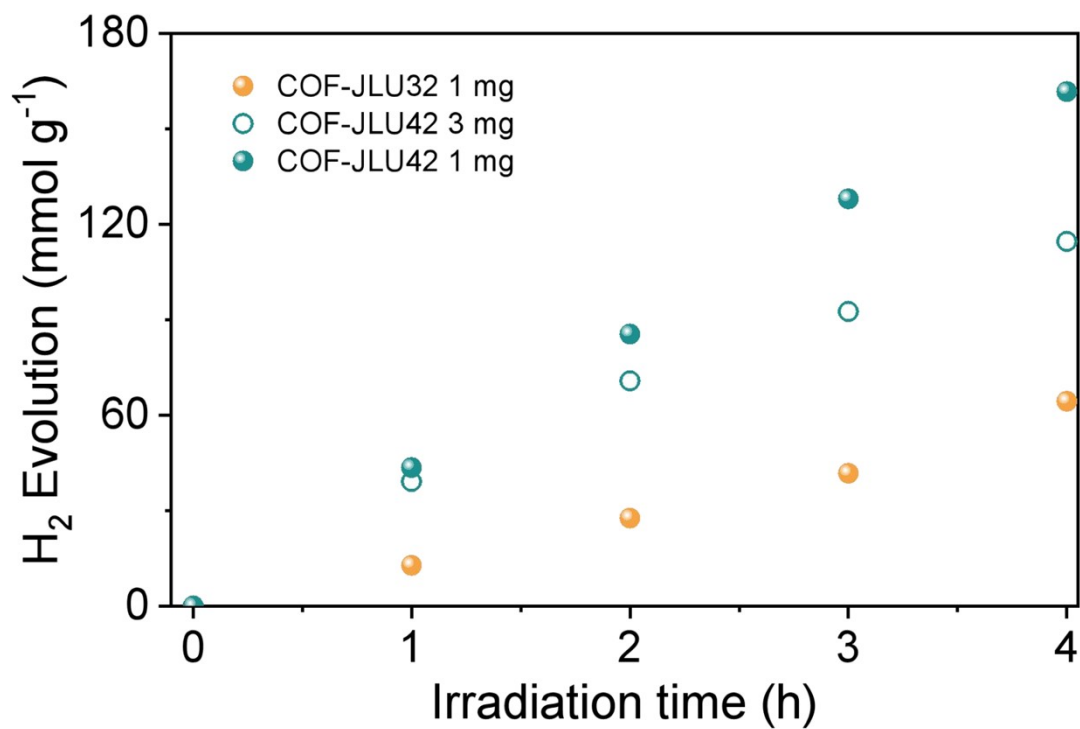


Figure S8. The photocatalytic H₂ evolution rate with different mass (1 and 3 mg) of COF-JLU42 and COF-JLU32 (1 mg) in the optimized reaction conditions (50 mL of H₂O, 3 wt% Pt, 0.1 M AA as SED, 420 < λ < 780 nm).

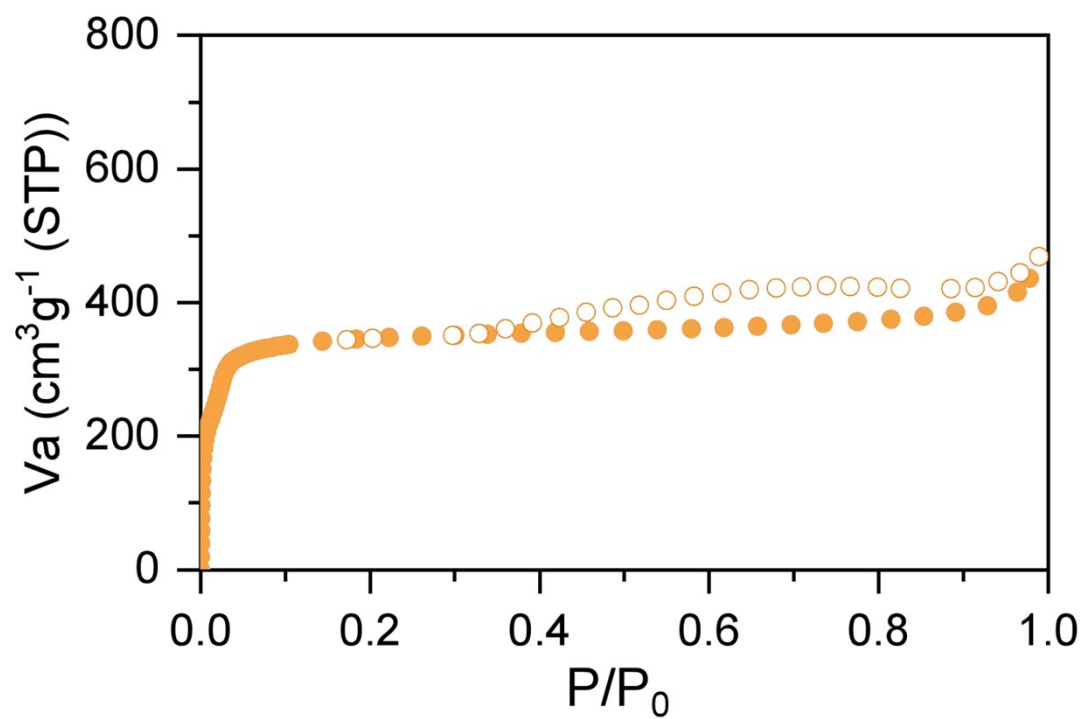


Figure S9. Nitrogen sorption isotherm curves of COF-JLU32.

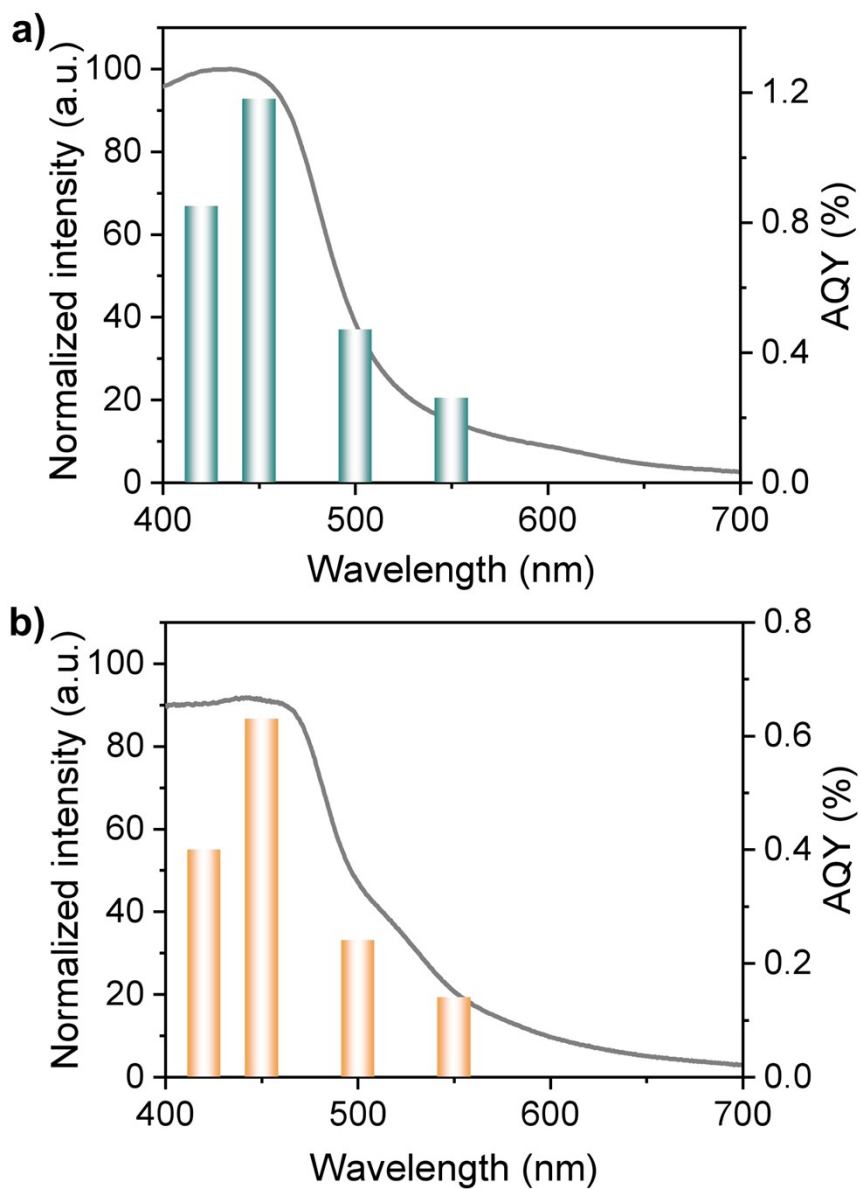


Figure S10. The AQY of COF-JLU42 (a) and COF-JLU32 (b) at four different incident light wavelengths for photocatalytic H₂ evolution in the optimized reaction conditions (10 mg of catalyst in 50 mL of H₂O, 3 wt% Pt, 0.1M AA as SED, $\lambda = 420$ nm, 450 nm, 500 nm and 550 nm, respectively).

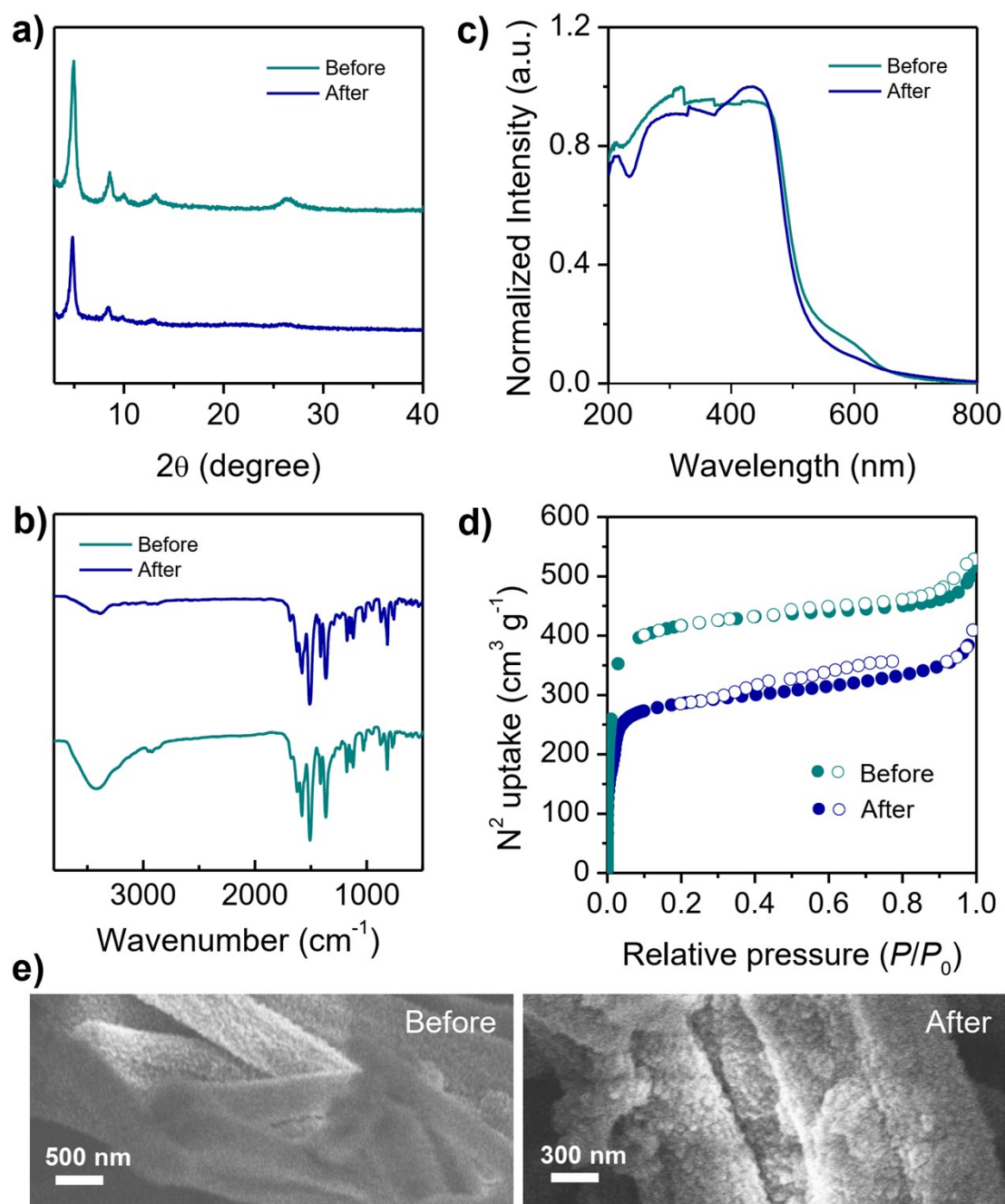


Figure S11. (a) PXRD curves, (b) UV-Vis DRS pattern, (c) FT-IR spectra, (d) Nitrogen sorption isotherm curves (Before: $1375 \text{ m}^2 \text{ g}^{-1}$; After: $1004 \text{ m}^2 \text{ g}^{-1}$), SEM images of COF-JLU42 before and after five runs for photocatalytic hydrogen evolution.

Table S1. Model Structures for COF-JLU42 were generated in BIOVIA Materials Studio. The unit cell, space group, lattice parameters, atom positions were showed below.

Space group: P-6			
a=b=22.0106 Å, c=3.5373 Å			
$\alpha=\beta=90^\circ, \gamma=120^\circ$			
Atom	x (Å)	y (Å)	z (Å)
C1	0.62171	0.42988	0.5
C2	0.64812	0.38521	0.5
N3	0.29874	0.5936	0.5
C4	0.48678	0.63304	0.5
C5	0.5254	0.59842	0.5
C6	0.37226	0.63167	0.5
C7	0.37896	0.52134	0.5
C8	0.41753	0.48668	0.5
O9	0.51282	0.30181	0.5
C10	0.59611	0.31519	0.5
C11	0.54902	0.39139	0.5
C12	0.50487	0.42372	0.5
C13	0.49116	0.52517	0.5
C14	0.41315	0.59491	0.5
N15	0.53224	0.49129	0.5

Table S2. The HER comparison of both COF-JLU42 with the other representative COF-based photocatalysis systems. The COF examples are selected to give the HER values using the mass-normalized unit of $\mu\text{mol h}^{-1} \text{g}^{-1}$.

Entry	Co-catalyst	SED	Light source	Intensity (mW cm^{-2})	COF (mg)	HER ($\mu\text{mol h}^{-1} \text{g}^{-1}$)	Ref.
COF-JLU42	Pt (3wt%)	AA	> 420 nm	160	1	40430	This work
COF-JLU32	Pt (3wt%)	AA	> 420 nm	160	1	16080	This work
N ₃ -COF	Pt (0.68wt%)	TEOA	> 420 nm	n/d	5	1703	Nat.Comm.,2015,6,8508
TpPa-COF-(CH ₃) ₂	Pt (3wt%)	SA	> 420 nm	n/d	5	8330	ChemCatChem,2019, 11, 2313
BtCOF150	Pt (1wt%)	TEOA	>420 nm	n/d	20	750	J. Am. Chem. Soc., 2020, 142, 9752-9762.
TtaTfa	Pt (8wt%)	AA	>420 nm	n/d	3	20700	Angew. Chem. Int. Ed.,2021, 60, 19797.
TP-TTA/SiO ₂ -1	Pt (3wt%)	AA	>420 nm	n/d	50	153200	CCS Chem., 2022, 4(7): 2429-2439.
RuCOF-TPB	Pt (2.76wt%)	AA	>420 nm	n/d	5	20308	Angew. Chem. Int. Ed.,2022, 134, e202208791
Co/Zn-Salen-COF	Pt (3wt%)	AA	>420 nm	n/d	10	1378	Angew. Chem. Int. Ed., 2023, 135, e202214143.
COF-923-AC	Pt (3wt%)	AA	>350 nm	n/d	5	23400	Angew. Chem. Int. Ed., 2023, 135, e202216073.
PIm-COF2	Pt (3wt%)	AA	>420 nm	n/d	5	7417	ACS Appl. Energy Mater.,2023, 6, 2, 1126–1133
TM-DMA-COF	Pt (3wt%)	AA	>420 nm	n/d	-	4300	Chin. J. Catal., 2023, 47: 171-180.
Py-HMPA	Pt (7wt%)	AA	>420 nm	n/d	30	37925	Appl. Catal., B, 2023, 338: 123074.
Zi-VCOF-1	Pt (3wt%)	AA	>420 nm	n/d	2	13457	ACS Appl. Mater.Interfaces,2023, 15, 31, 37845–37854
COF-954	Pt (5wt%)	AA	>420 nm	n/d	5	137226	Adv. Mater., 2023, n/a, 2308251.
PABZ-TP	Pt (0.5wt%)	AA	>420 nm	n/d	1	115000	Chin. J. Catal., 2023, 48, 137-149.

Section 3. References

1. G. Li, P. Fu, Q. Yue, F. Ma, X. Zhao, S. Dong, X. Han, Y. Zhou and J. Wang, *Chem Catal.*, 2022, **2**, 1734-1747.
2. Z. Lin, S. Liu, W. Weng, C. Wang and J. Guo, *Small*, 2023, **n/a**, 2307138.
3. R. B. Ferreira, J. M. Figueroa, D. E. Fagnani, K. A. Abboud and R. K. Castellano, *Chem. Commun.*, 2017, **53**, 9590-9593.
4. H. Wei, J. Ning, X. Cao, X. Li and L. Hao, *J. Am. Chem. Soc.*, 2018, **140**, 11618-11622.
5. R. Gomes, P. Bhanja and A. Bhaumik, *Chem. Commun.*, 2015, **51**, 10050-10053.